

A Microbial Survey of Lake Kivu: Mechanisms of Nitrogen Cycling

by
Kaitlyn Przydzial

Submitted to the Department of Earth, Atmospheric, and Planetary Sciences

in partial fulfillment of the requirements for the degree of
Bachelor of Science in Earth, Atmospheric, and Planetary Sciences
at the

MASSACHUSETTS INSTITUTE OF TECHNOLOGY

June 2023

©Kaitlyn Przydzial. All rights reserved.

The author hereby grants to MIT a nonexclusive, worldwide, irrevocable, royalty-free license to exercise any and all rights under copyright, including to reproduce, preserve, distribute and publicly display copies of the thesis, or release the thesis under an open-access license.

Author
Department of Earth, Atmospheric, and Planetary Sciences
May 19, 2023

Certified by.....
Roger E. Summons
Schlumberger Professor of Geobiology
Thesis Supervisor

Certified by.....
Benjamin Uveges
Postdoctoral Associate
Thesis Supervisor

Accepted by
Thomas A. Herring
Chair, Committee on Undergraduate Program

A Microbial Survey of Lake Kivu: Mechanisms of Nitrogen Cycling

by

Kaitlyn Przydzial

Submitted to the Department of Earth, Atmospheric, and Planetary Sciences
on May 19, 2023, in partial fulfillment of the
requirements for the degree of
Bachelor of Science in Earth, Atmospheric, and Planetary Sciences

Abstract

Ocean Anoxic Events (OAEs) are periods in Earth's history during which large portions of the oceans contain decreased amounts of oxygen. OAEs can be very difficult to study since modern oceans are generally well-oxygenated. Here Lake Kivu, a meromictic lake with deep anoxic layers, is presented as a potential OAE analogue and is used to study a proposed nitrogen cycling mechanism that could explain the characteristic $\delta^{15}\text{N}$ excursions associated with OAEs. Biomarkers are isolated from sediment samples and analyzed across depth below the lake floor. The results are consistent with a biologically mediated nitrogen cycling mechanism, shedding more light on a potential mechanism to explain nitrogen cycling in OAEs.

Thesis Supervisor: Roger E. Summons
Title: Schlumberger Professor of Geobiology

Thesis Supervisor: Benjamin Uveges
Title: Postdoctoral Associate

Acknowledgments

I would like to thank everyone in the Summons lab for their help in completing this project. Thank you all for your patience and kindness; I could always count on the fact that going into lab would make the project feel more attainable because there were so many people there willing to help. I would especially like to thank Ben Uveges, who has been extremely generous with his time and who has probably forgotten more about mass spectrometers than I will ever know.

I would also like to thank my parents, who are most of the reason I am even at MIT in the first place. Thanks for listening to me talk about this thesis even when I wasn't making much sense. Thanks to Aydin McPhilemy, Anna Needle, and Áine Playdon, who have let me hang out with them for almost a decade despite the fact that my name doesn't start with an A.

Finally, I would like to thank the entire MIT EAPS undergraduate community, particularly the Class of 2023 and Jane Abbott. This thesis could not have happened without your support (and commiseration).

Contents

1	Introduction	13
1.1	Setting	13
1.2	Microbial Community	16
1.3	Biomarkers	18
1.4	Motivation	18
2	Methods	21
2.1	Sample Collection	22
2.2	Core Samples	22
2.3	Laboratory Analysis	23
3	Results	25
3.1	Biomarker Characterization	25
3.2	Relative Abundance	27
3.3	Biomarker Ratios	33
3.4	Other Identified Compounds	34
4	Discussion	37
5	Conclusion	41
A	Figures	43

List of Figures

1-1	A large-scale map of Lake Kivu, which also displays areas of high volcanic activity [11].	13
1-2	The stratified layers of Lake Kivu [12].	14
1-3	TOC, isotope, and pigment ratio data from the core sample studied in this project [12].	16
1-4	A high-resolution visible light scan of a section of the 13A sediment core aligned with a stratigraphic column for the region.	17
2-1	A map showing the location of 13-13AB.	21
2-2	High-resolution visible light scans of relevant portions of the 13A core sample.	23
3-1	Chromatogram for non-polar compounds at a depth of 137.5cm	25
3-2	Chromatogram for non-polar compounds at a depth of 215cm	26
3-3	Chromatogram for polar compounds at a depth of 148cm	26
3-4	Chromatogram for polar compounds at a depth of 203.5cm	27
3-5	A heat map showing the abundance of non-polar compounds found in the core section 13A-2 relative to the largest peak detected in each sample.	28

3-6	A heat map showing the abundance of non-polar compounds found in the core section 13A-3 relative to the largest peak detected in each sample.	28
3-7	A heat map showing the abundance of non-polar compounds found in the core section 13A-4 relative to the largest peak detected in each sample.	29
3-8	A heat map showing the abundance of polar compounds found in the core section 13A-2 relative to the largest peak detected in each sample.	29
3-9	A heat map showing the abundance of polar compounds found in the core section 13A-3 relative to the largest peak detected in each sample.	30
3-10	A heat map showing the abundance of polar compounds found in the core section 13A-4 relative to the largest peak detected in each sample.	30
3-11	A heat map showing the relative abundance of non-polar compounds in core section 13A-3, using an n-alkane as a reference peak.	31
3-12	A heat map showing the relative abundance of polar compounds in core section 13A-3, using a sterol as a reference peak.	32
3-13	The ratios between major biomarker classes in each sample site.	33
3-14	The steroid/hopanooid ratios across depth in both the polar and non-polar fractions of core section 13A-3.	34
4-1	The bacterial and archaeal species present in Lake Kivu across layers [6].	39
4-2	The organisms and compounds associated with various $\delta^{13}\text{C}$ values [10].	40
A-1	Mass spectra from the polar fraction of core sample 4A that eluted at approximately 100 minutes.	43
A-2	Mass spectra from the non-polar fraction of core sample 3A showing a steroid, identified as Cholest-2-ene, that eluted at approximately 70 minutes.	44

A-3	Reference spectrum for Cholest-2-ene.	44
A-4	Mass spectra from the non-polar fraction of core sample 2A showing an n-alkane that eluted at approximately 58 minutes.	45
A-5	Mass spectra from the non-polar fraction of core sample 4A showing an n-alkane that eluted at approximately 58 minutes.	45
A-6	Mass spectra from the polar fraction of core samples 2A and 3A that eluted at approximately 80 minutes.	46
A-7	Mass spectra from the polar fraction of core samples 2A and 3A that eluted at approximately 86 minutes.	46
A-8	Mass spectra from the polar fraction of core sample 4A that eluted at approximately 89 minutes.	47

Chapter 1

Introduction

1.1 Setting

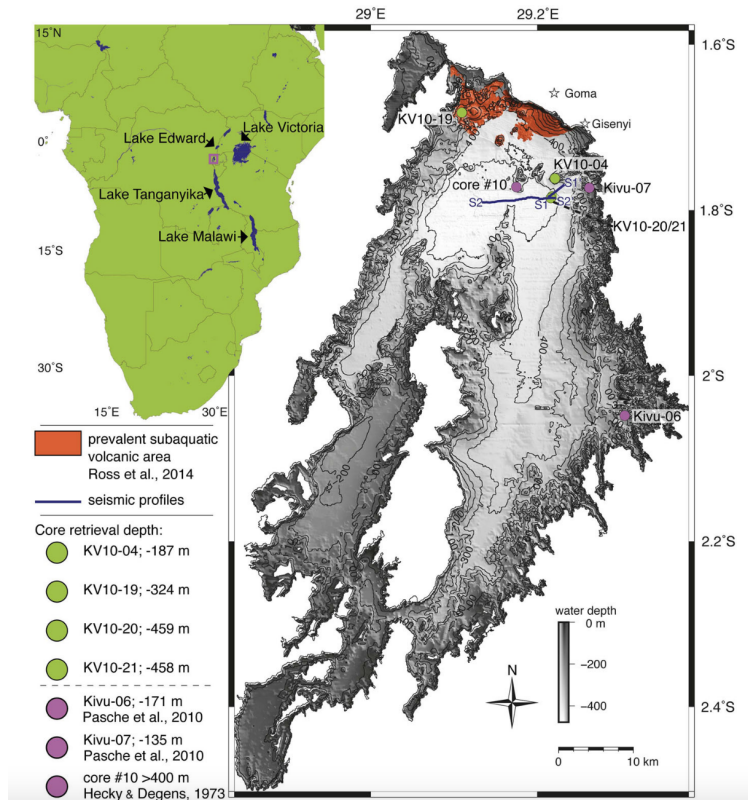


Figure 1-1: A large-scale map of Lake Kivu, which also displays areas of high volcanic activity [11].

Ocean Anoxic Events are periods in Earth’s history when large portions of the ocean become depleted of oxygen, leading to the accumulation of organic matter in sediments, the formation of black shales, and often heightened extinction rates [4]. The specific conditions that lead to OAEs are not well understood and modern oceans, which are generally well oxygenated [8], leave us with an imperfect comparison. In order to gain insight into these mechanisms, it is necessary to study modern environments that may serve as better analogues for OAEs. The unusual redox stratification of the East African Lake Kivu makes it a good candidate for such studies.

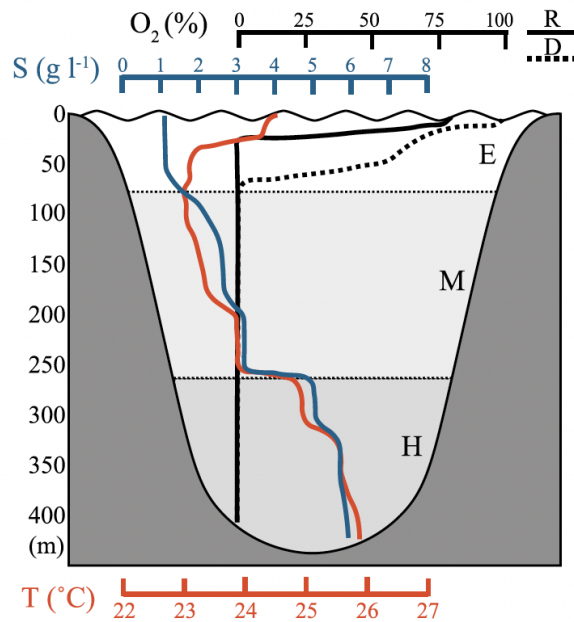


Figure 1-2: The stratified layers of Lake Kivu [12].

Lake Kivu is a meromictic lake located in the East African Rift Valley. The upper section (65m) of the lake experiences seasonal mixing but the waters below that are permanently stratified and anoxic. In particular, it has a deep anoxic layer that is rich in nutrients, especially ammonium (NH₄⁺) and methane (CH₄). Nutrient circulation within the lake is largely driven by an inflow of spring water that occurs at a depth of 250 meters [2]. Most biological activity in Lake Kivu happens in the photic zone; the inflow of spring water drives nutrients toward the surface, where they become

available for biological use [12].

Lake Kivu has been significantly impacted by volcanic activity. An eruption in the late Pleistocene blocked the outlet of the lake, leading to a rise in the water level that, in combination with hydrothermal activity deep in the lake, caused the water column stratification observed today [11]. The lake experiences ongoing volcanic activity, largely in the form of hydrothermal springs. These springs contribute to the large amounts of CH_4 present in the deepest parts of Lake Kivu.

Lake Kivu is a good analogue for Ocean Anoxic Events for a number of reasons. Not only does it have largely anoxic waters but it also displays geochemical signals characteristic of OAEs. These signals include negative $\delta^{13}\text{C}$ and $\delta^{15}\text{N}$ excursions along with an elevated TOC, all of which are seen in the Kivu data shown in Figure 1-3. The focus of this project is the negative $\delta^{15}\text{N}$ excursions. The mechanisms behind these $\delta^{15}\text{N}$ excursions are not fully understood; the problem is made particularly difficult since they do not occur in many modern environments. Previous study of Lake Kivu has suggested that the delivery of NH_4^+ to surface waters and its subsequent utilization by phytoplankton may lead to the production of $\delta^{15}\text{N}$ -depleted organic matter that is then deposited in sediments following these nutrient mixing events. This mechanism could also explain the $\delta^{15}\text{N}$ excursions observed in OAEs and thus warrants further study.

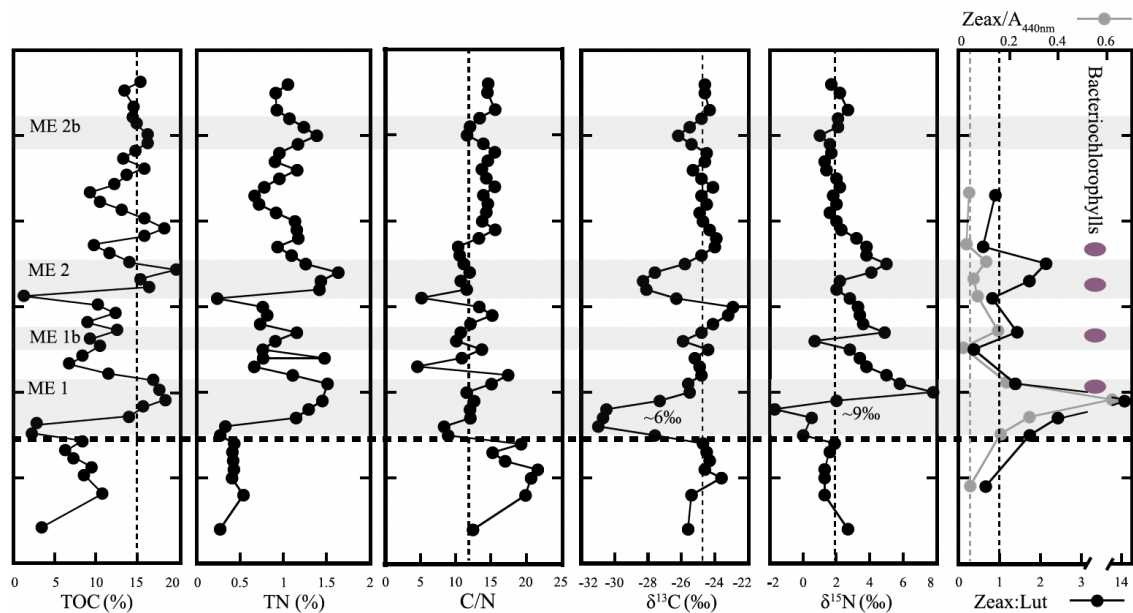


Figure 1-3: TOC, isotope, and pigment ratio data from the core sample studied in this project [12].

1.2 Microbial Community

Many biological surveys have been carried out in Lake Kivu, revealing a great deal about the microbial ecosystem of the environment. The mechanism proposed to explain the $\delta^{15}\text{N}$ excursion shown in Figure 1-3 involves ammonium uptake by planktonic organisms in the upper part of Lake Kivu. Similar excursions associated with OAEs have been interpreted as being due to contribution from nitrogen-fixing cyanobacteria [4]. When examining lake floor sediments that preserve a mixing event, it is thus helpful to understand the microbial populations that may have been involved in the deposition of organic matter.

Lake Kivu contains a wide variety of microorganisms: bacteria, archaea, and small eukaryotes are all present. The abundance of each group changes across the lake's depth. In the oxic uppermost layer, bacteria are the most abundant microorganism with only small amounts of archaea being present. As depth increases, archaea become

slightly more abundant but are still significantly outnumbered by bacteria [7]. In the photic layer, the microbial population is dominated by diatoms, cyanobacteria, and cryptophytes. The relative abundances of the groups change with seasonal variation but remain overall dominant. The eukaryote population is largely composed of six classes: Stramenopiles (21.4%), Alveolata (21.4%), Cryptophyta (14.3%), Chytridiomycota (8.9%), Kinetoplastea (7.1%) and Choanoflagellida (5.4%) [6].

The overall microbial population of Lake Kivu is important to fully understand the nitrogen cycling mechanism we are investigating. However, it is also important to consider the microbial populations already known to be in the sediment samples around which this study centers (Core 13A). As seen in Figure 1-4, two diatomite layers are present in the core sample, one at a depth of 137 cm and one at 144 cm. There are also five sapropel layers, located at depths of 127 cm, 129 cm, 133 cm, 135 cm, and 143 cm.

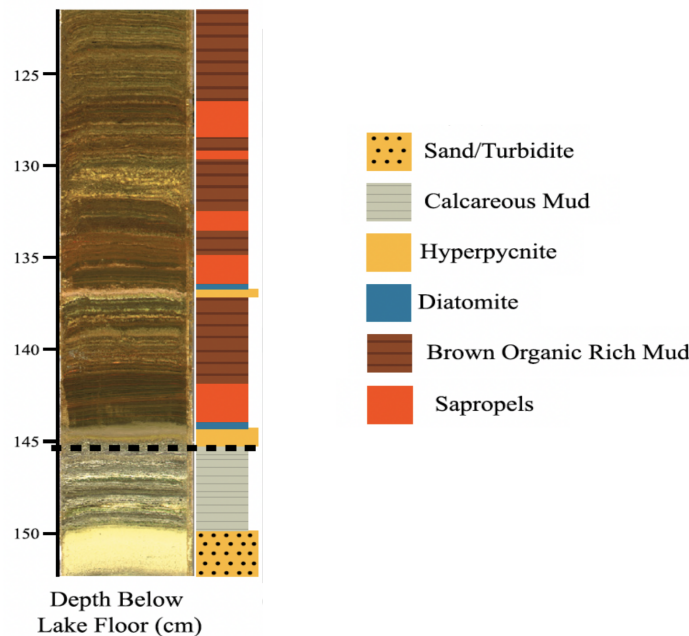


Figure 1-4: A high-resolution visible light scan of a section of the 13A sediment core aligned with a stratigraphic column for the region.

1.3 Biomarkers

Biomarkers are molecular fossils that are preserved in the rock and sedimentary record. They are produced by living organisms and generally change very little through preservation. Since biomarkers are structurally analogous to their precursor lipids, it is often possible to determine a great deal about their origins based solely on chemical structure. In some cases, biomarkers can be diagnostic of a particular organism. However, biomarkers can still reveal useful information about their sources even if a less specific identification is made. In this study, we observed largely alka(e)ne, steroidal, and hopanoid biomarkers. While alka(e)nes are present in a large number of organisms, details such as carbon number can significantly narrow down potential sources. Steroids and hopanoids are both more specific and occur almost exclusively in eukaryotes and bacteria, respectively [10].

Recent work in Lake Kivu has resulted in the identification of carotenoid and chlorophyll biomarkers in sediment samples from Core 13A. The carotenoids detected include zeaxanthin, which is generally associated with green algae, and lutein, which is generally associated with cyanobacteria. The chlorophyll biomarkers include bacteriochlorophyll derivatives, which are commonly associated with green sulfur bacteria, purple sulfur bacteria, and purple non-sulfur bacteria [12].

1.4 Motivation

Recent geochemical work done in Lake Kivu suggests that biological effects may play a part in the $\delta^{15}\text{N}$ excursion seen in the sediment core. While that study also found some potential evidence of biological involvement in the form of carotenoid and chlorophyll derivatives, biomarker analysis was not the primary goal. This study seeks to re-examine those sediments and better qualify the diversity of biomarkers present in the samples. We are particularly interested in evaluating samples from depths

associated with the mixing event. Since the density stratification and deep anoxic waters in Lake Kivu make the lake a good analogue for the study of OAEs, a better understanding of the nitrogen cycling mechanism in Lake Kivu could potentially be extended to the $\delta^{15}\text{N}$ excursions associated with anoxic oceans.

Chapter 2

Methods

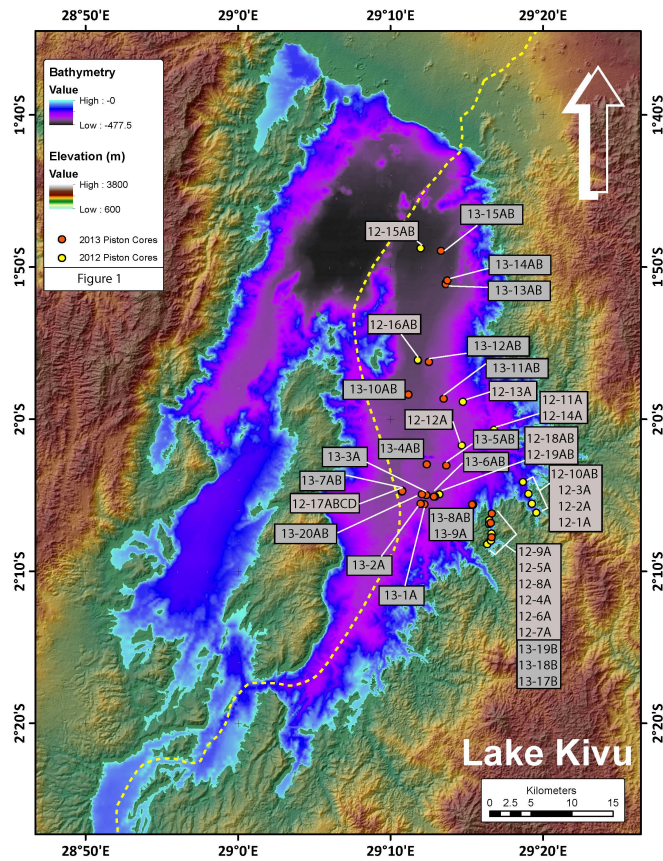


Figure 2-1: A map showing the location of 13-13AB.

2.1 Sample Collection

The samples used for these experiments were collected in March of 2013 aboard the R/V Kilindi in association with the Lake Kivu Monitoring Programme. They were collected from the Northern Basin of Lake Kivu, at the point labeled 13-3A in Figure 1-5. That point corresponds to a GPS location of $29^{\circ}13'37.9''\text{E}$, $1^{\circ}51'3.4''\text{S}$, and a water depth of 427 m. Coring was carried out utilizing a modified Kullenberg piston coring system equipped with a 380 kg driving weight, in 7 cm diameter polycarbonate tubes. After collection, cores were stored at 3°C until split and sampled.

2.2 Core Samples

The full 13A core was separated into several sections and high-resolution visible light scans were taken of each one (Figure 2-2). 13A-2, 13A-3, and 13A-4 are all taken from the same core but cover different depths of the core. 13A-2 is the shallowest section, covering a depth of 54.5 to 86.5 cm. 13A-3 follows, stretching from 133 to 149 cm. 13A-4 is at the bottom of the column, stretching from 203.5 to 272 cm. Each section was then further subsampled before being run through laboratory analysis.

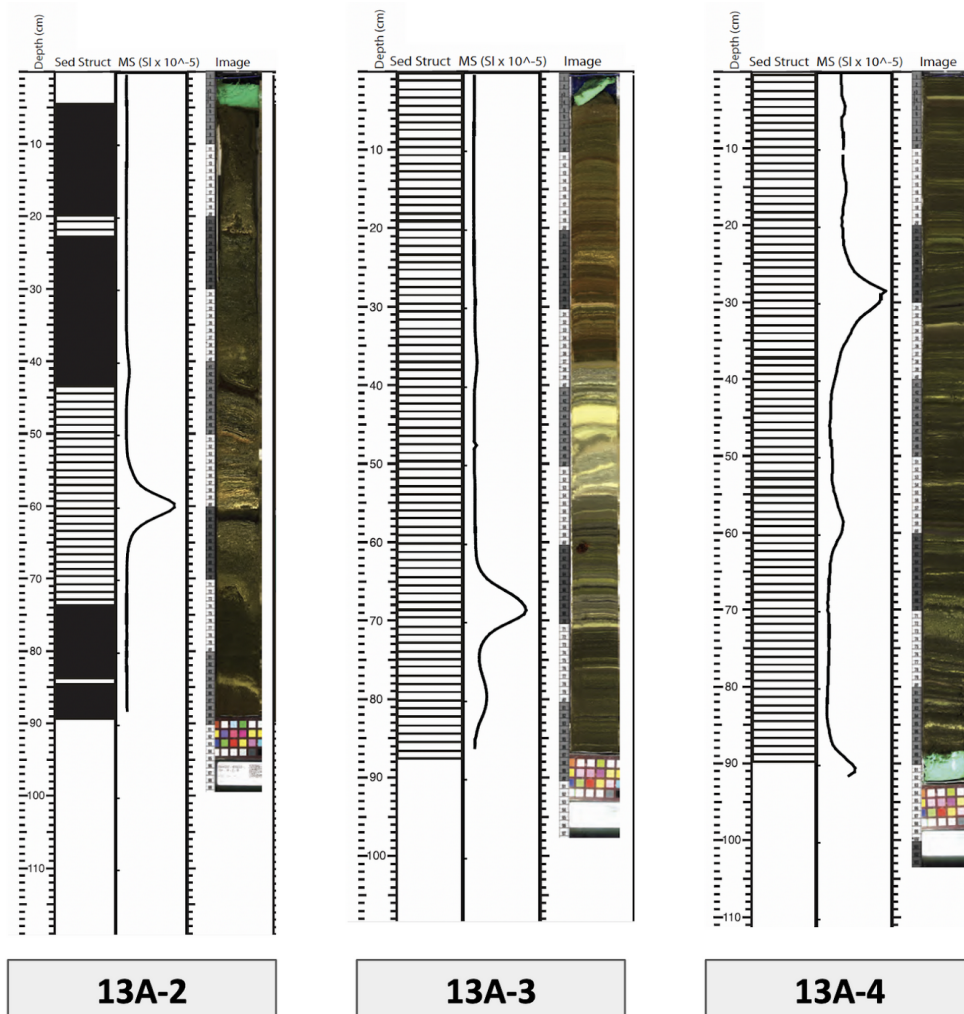


Figure 2-2: High-resolution visible light scans of relevant portions of the 13A core sample.

2.3 Laboratory Analysis

The total lipid extract was obtained from all samples and split into polar and non-polar fractions on small silica gel columns. The polar fractions were taken up in pyridine and heated at 37°C with BSTFA for one hour to create TMS-derivatives. The fractions were run on an Agilent 5975C Inert MSD with Triple-Axis Detector on an Agilent DB-5 column using a 105 minute method with temperature ramp in

full scan mode. Analysis of data was completed on the Agilent MassHunter software, using published reference spectra to identify compounds.

Chapter 3

Results

3.1 Biomarker Characterization

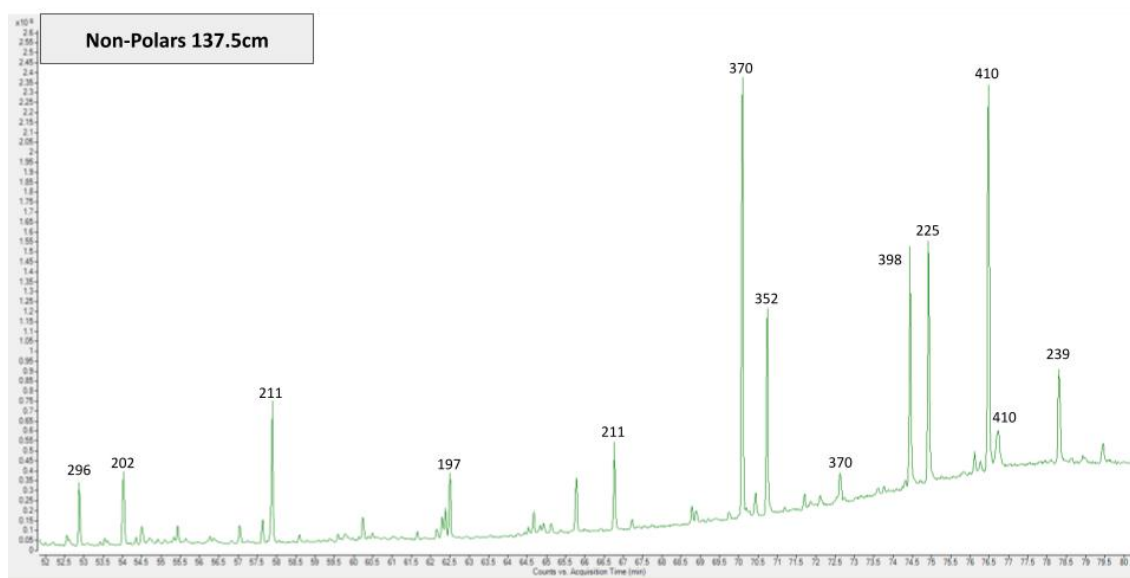


Figure 3-1: Chromatogram for non-polar compounds at a depth of 137.5cm

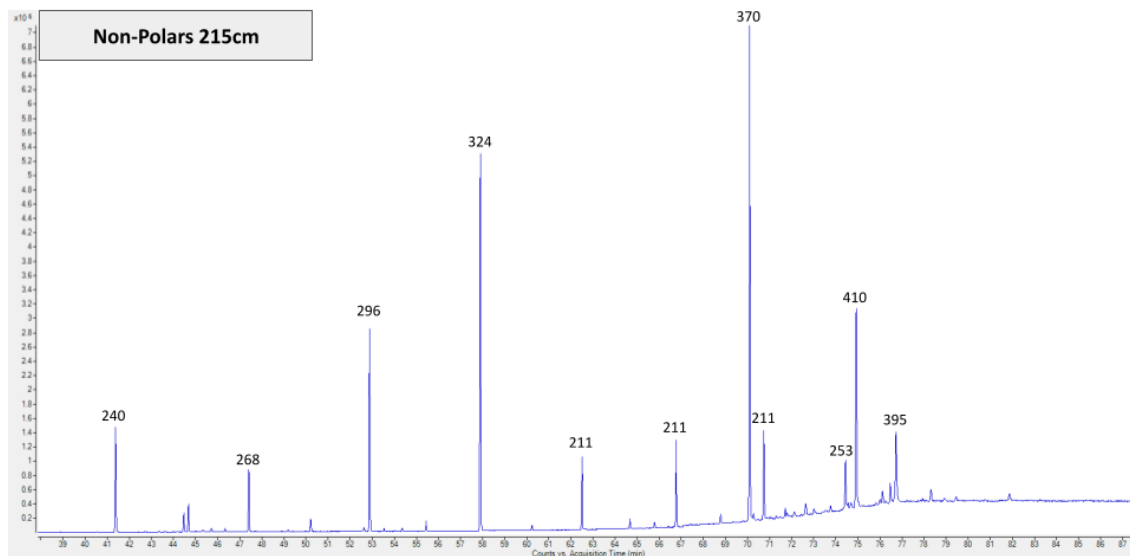


Figure 3-2: Chromatogram for non-polar compounds at a depth of 215cm

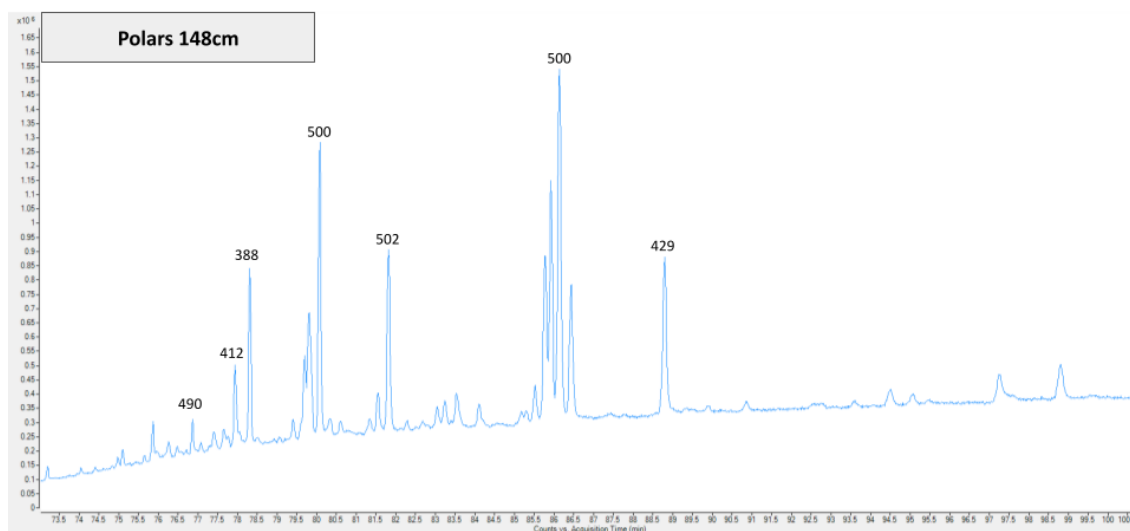


Figure 3-3: Chromatogram for polar compounds at a depth of 148cm

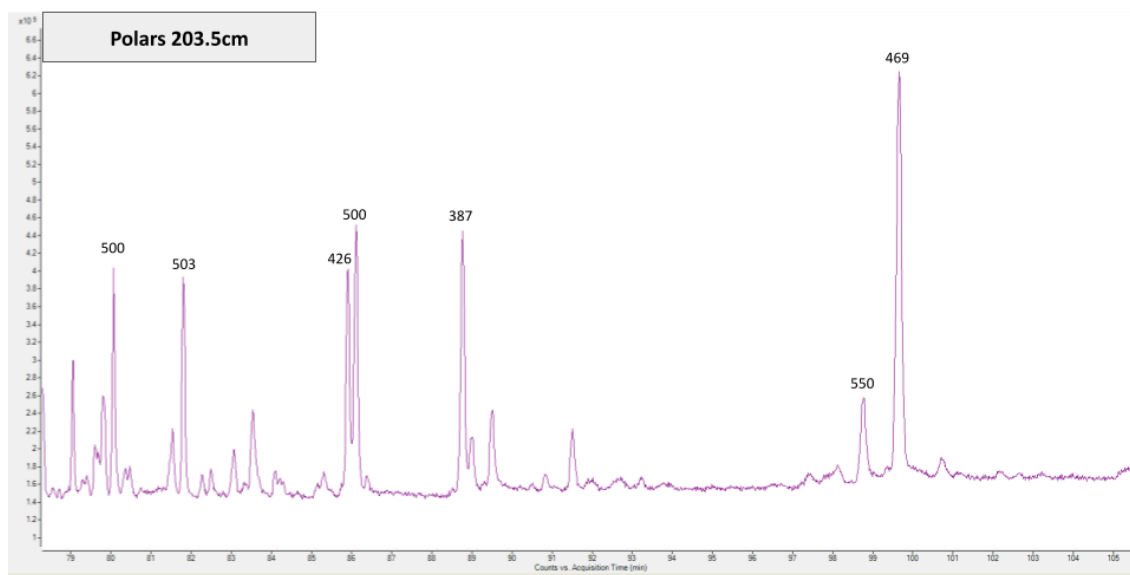


Figure 3-4: Chromatogram for polar compounds at a depth of 203.5cm

Representative chromatograms were collected from across the core sample and each peak was labeled with the molecular mass of the corresponding compound. Mass spectra for some of the most abundant compounds are included in the Appendix.

3.2 Relative Abundance

Eight heat maps were generated displaying the relative abundances of the biomarkers found at each of the sample sites, divided into polar and nonpolar fractions. In Figures 3-5 — 3-10, abundances are calculated relative to the largest peak detected in each sample's chromatogram. These figures show which biomarkers are most prevalent in each sample and provide insight into how the most abundant class of compound changes across depth. The abundances in Figures 3-11 and 3-12 are calculated relative to a reference peak selected from each chromatogram. Reference peaks were selected from the pool of compounds that were present in every sample at a given site. These figures provided more information on how the abundance of individual compounds,

especially those most present in the samples, change over depth.

Abundances are represented by color; darker colors represent more abundant compounds. The columns are organized in order of increasing retention time and are labeled with the broad class of biomarker (alka(e)ne, sterane, hopane) to which each compound belongs. While only the broad class of compound is shown in the figures above, more specific identifications were made for many of the compounds and checked for consistency across samples.

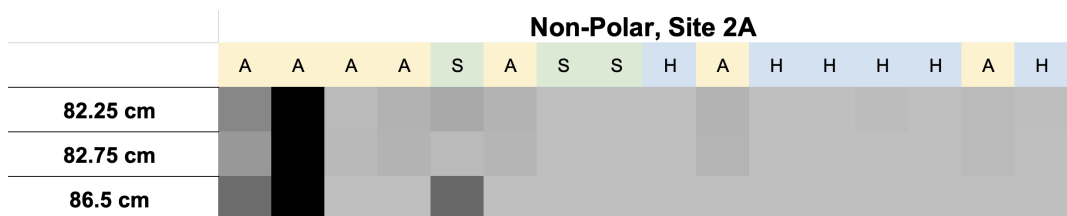


Figure 3-5: A heat map showing the abundance of non-polar compounds found in the core section 13A-2 relative to the largest peak detected in each sample.

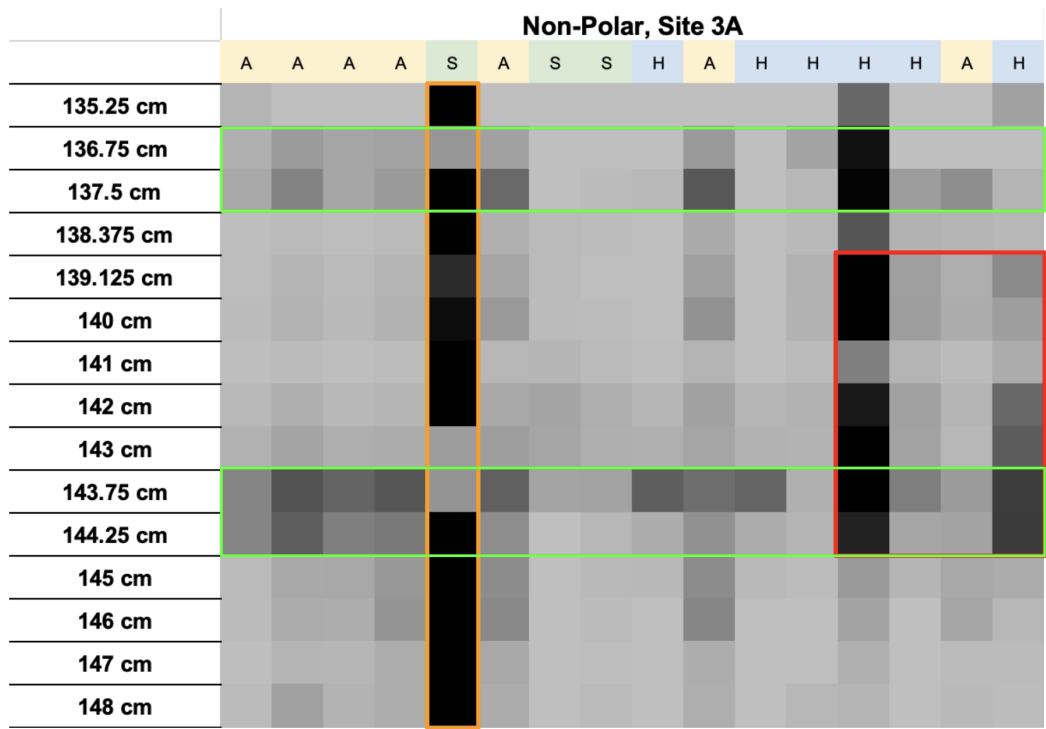


Figure 3-6: A heat map showing the abundance of non-polar compounds found in the core section 13A-3 relative to the largest peak detected in each sample.

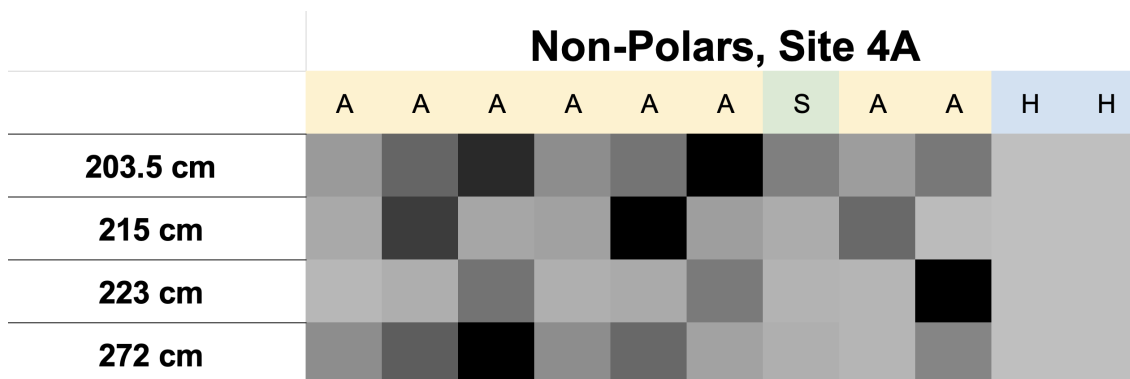


Figure 3-7: A heat map showing the abundance of non-polar compounds found in the core section 13A-4 relative to the largest peak detected in each sample.

Figures 3-5 — 3-7 show the abundance of compounds in the nonpolar samples relative to the highest chromatogram peak detected in each sample. Thus, the darkest spots represent compounds that are most abundant in each sample relative to the other compounds detected in the sample. Data from both core section 13A-2 and core section 13A-4 show that alka(e)nes are the most abundant biomarkers detected in most of the samples. Core section 13A-3 shows a mix of abundant compound types, though the most abundant compounds are all hopanoids and steroids. This section also contains several areas of interest, which have been surrounded by colored boxes. The green boxes surround the depths corresponding to diatomite layers previously identified in the sediment, the red box surrounds the depths corresponding to the mixing event, and the orange box surrounds a steroid, identified as Cholest-2-ene, that appears to be consistently abundant across much of section 13A-3.

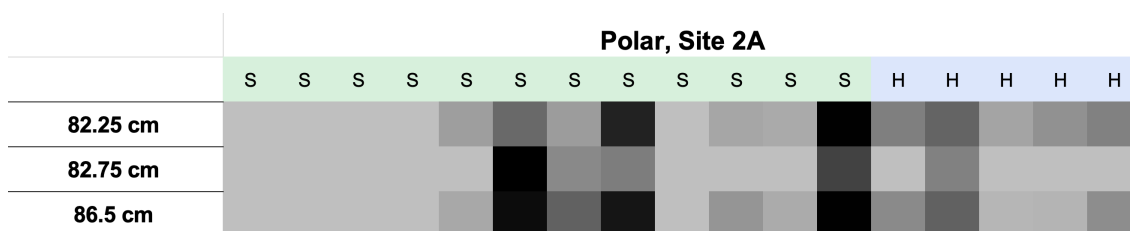


Figure 3-8: A heat map showing the abundance of polar compounds found in the core section 13A-2 relative to the largest peak detected in each sample.

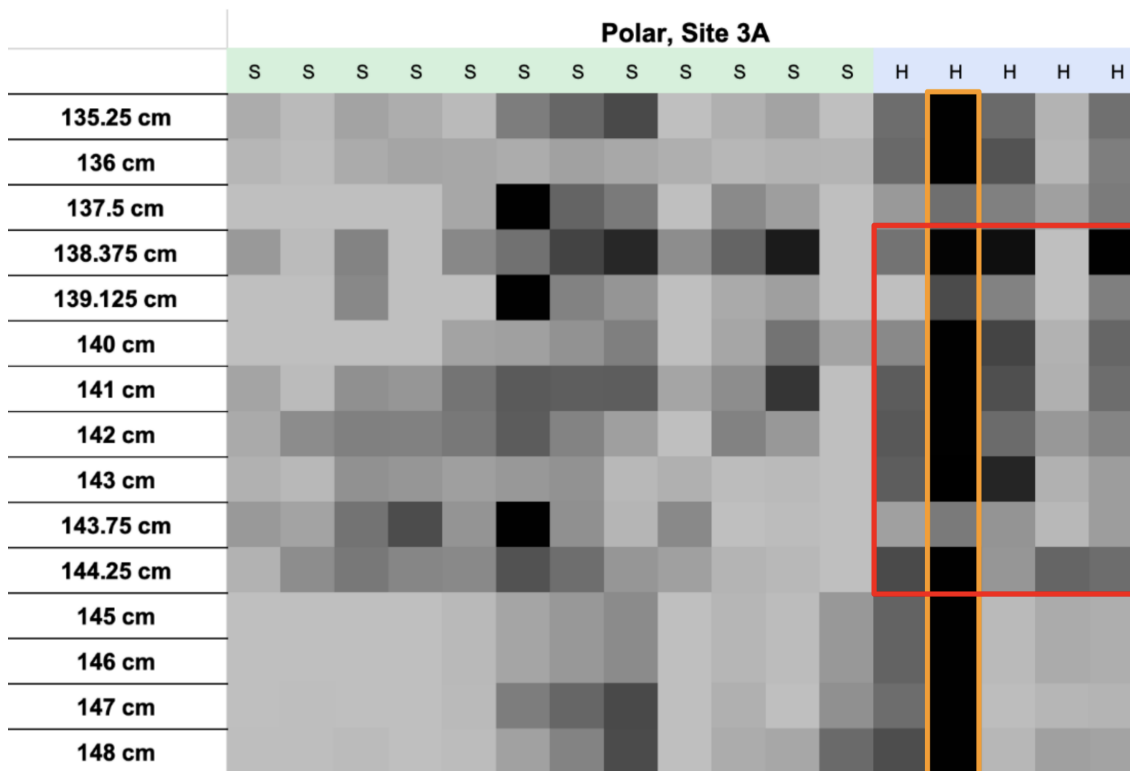


Figure 3-9: A heat map showing the abundance of polar compounds found in the core section 13A-3 relative to the largest peak detected in each sample.

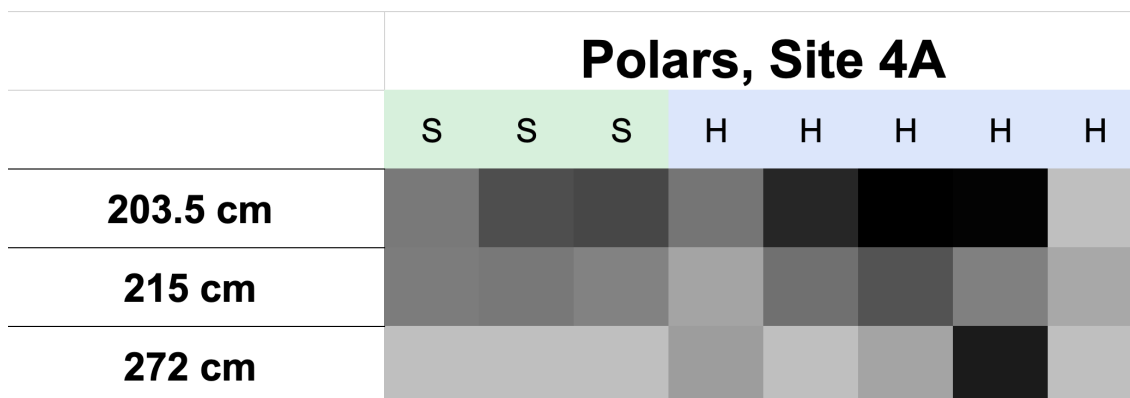


Figure 3-10: A heat map showing the abundance of polar compounds found in the core section 13A-4 relative to the largest peak detected in each sample.

Figures 3-8 — 3-10 show the abundance of compounds in the polar samples relative to the highest chromatogram peak detected in each sample. The samples from core section 13A-2 appear to be dominated by sterols, while sections 13A-3 and 13A-4 appear to have a mix of sterols and hopanols. One hopanol in section 13A-3 is

consistently one of the most abundant across the entire depth of the section.

Two additional heat maps, Figures 3-11 and 3-12, were generated to better explore some areas of interest discovered in Figures 3-5 — 3-10. In the following heat maps, the abundances of each compound were calculated relative to a reference peak that was present across the entire depth of the section. This calculation allows for a more detailed view of some of the more abundant compounds in the heat maps shown above.

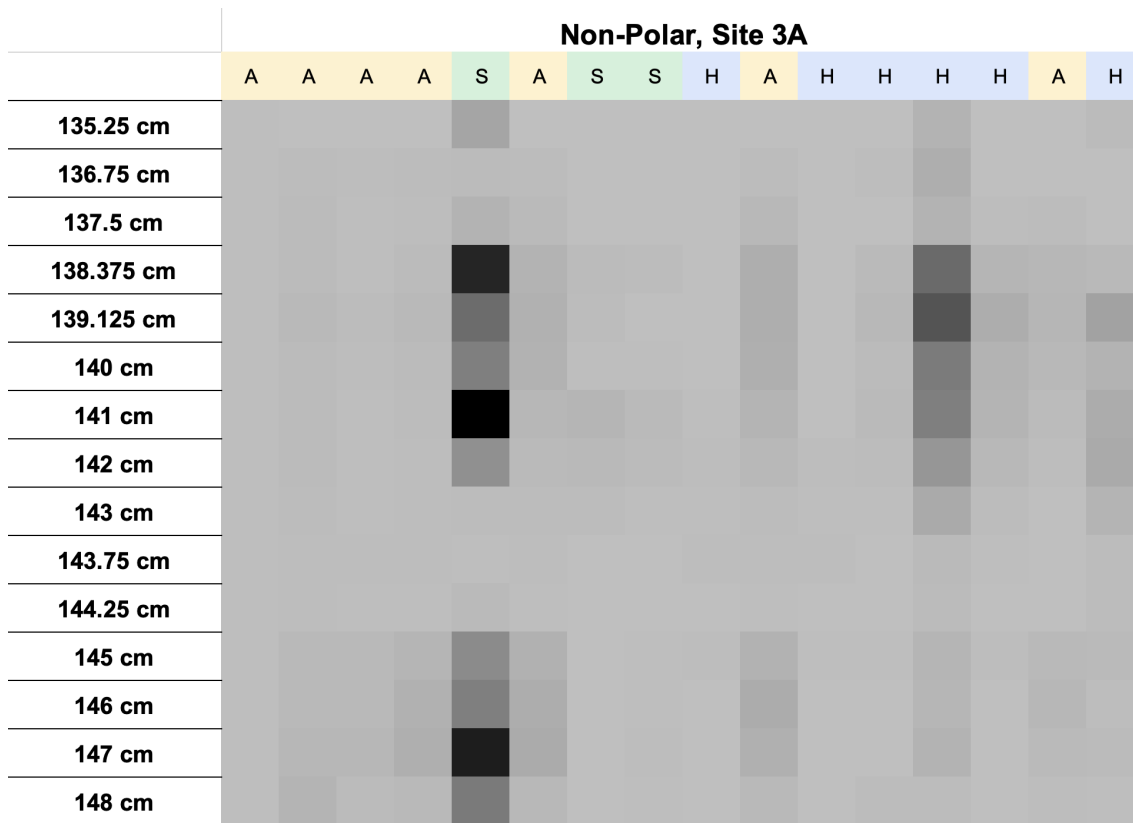


Figure 3-11: A heat map showing the relative abundance of non-polar compounds in core section 13A-3, using an n-alkane as a reference peak.

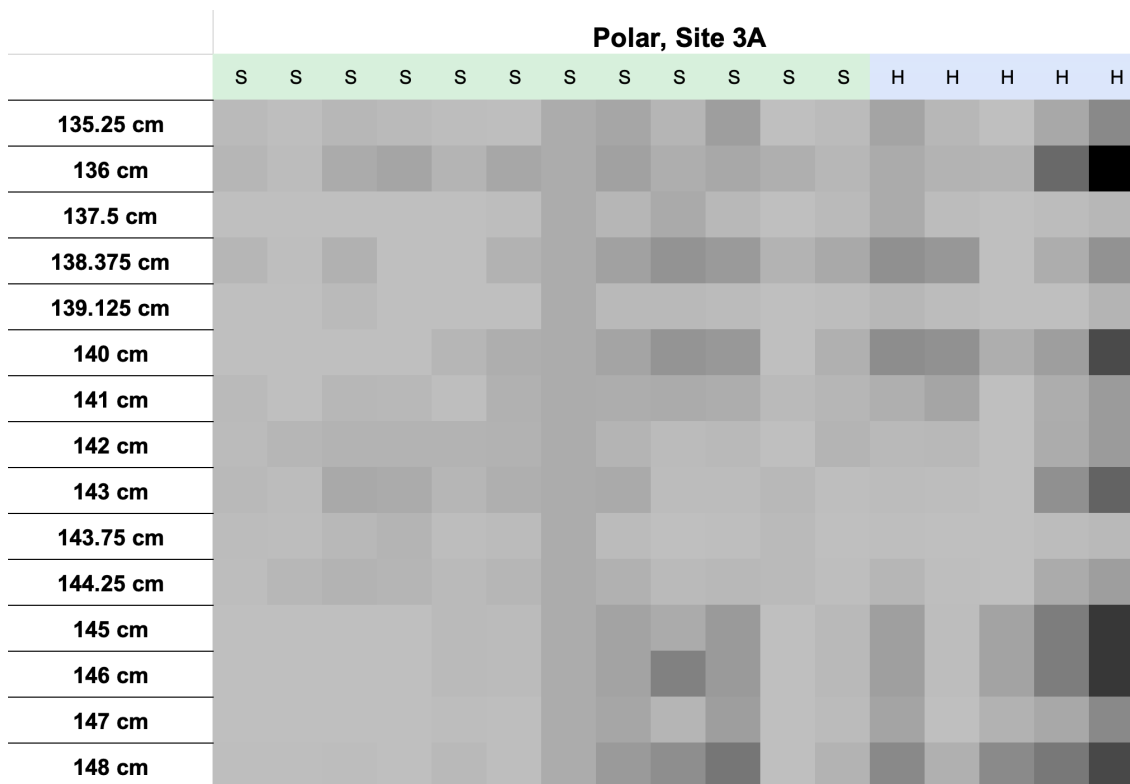


Figure 3-12: A heat map showing the relative abundance of polar compounds in core section 13A-3, using a sterol as a reference peak.

In Figure 3-11, a steroid and hopanoid are both shown to be significantly more abundant than the reference n-alkane. However, the relative abundances do change across depth. In Figure 3-12, two hopanols are shown to be noticeably more abundant than the reference sterol. Several other sterols in the sample seem to be approximately equally abundant to the reference sterol. These relative abundances also change across depth.

3.3 Biomarker Ratios

	Steroid/ Hopanoid	Hopanoid/ Alka(e)ne	Alka(e)ne/ Steroid
Non-Polars, Section 13A-2	15.251	0.00912	7.1888
Non-Polars, Section 13A-3	1.160863086	1.028565107	0.83750462
Non-Polars, Section 13A-4	0.6896143	0.33849921	4.28386797
Polars, Section 13A-2	0.80165086	—	—
Polars, Section 13A-3	0.8645993	—	—
Polars, Section 13A-4	1.132179	—	—

Figure 3-13: The ratios between major biomarker classes in each sample site.

Figure 3-13 shows the ratios between major biomarker classes in each sample site for both the polar and non-polar fractions. There is no consistent pattern governing the changes across depth. However, among the sections for which multiple ratios were able to be calculated, the hopanoid/alka(e)ne ratio is always the lowest value. The three ratios are significantly different in sections 13A-2 and 13A-4 but are similar in 13A-3. Similarly, the steroid/hopanoid ratio calculated for each of the polar sections shows that the ratio stays relatively consistent across the entire sampled depth of the core. The nonpolar steroid/hopanoid ratio for the 13A-3 section of the core is also similar to the consistent polar ratio. It is worth noting that the data for the non-polar fractions of section 13A-2 was relatively noisy and thus the calculations shown in this table may not be fully accurate.

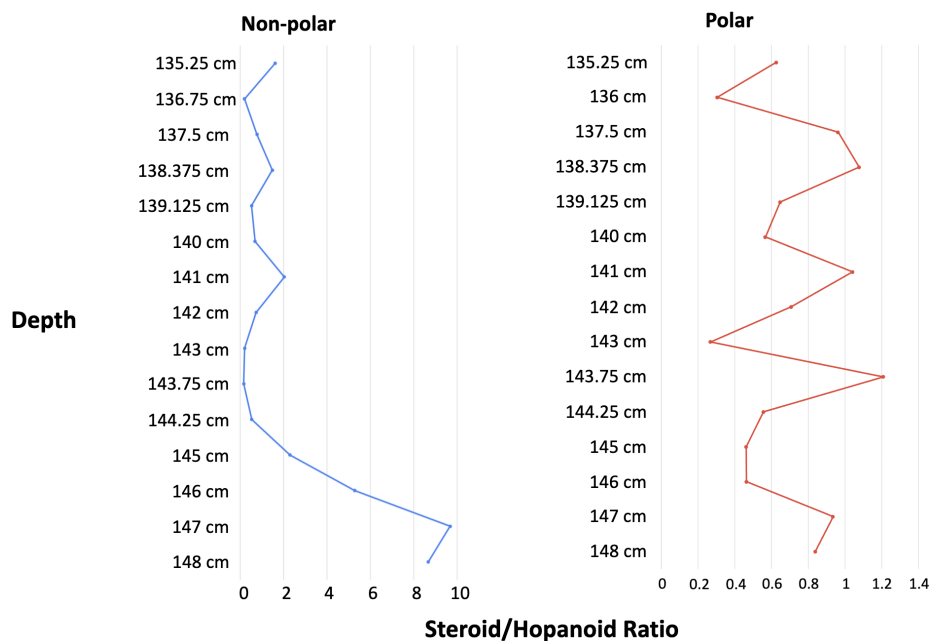


Figure 3-14: The steroid/hopanoid ratios across depth in both the polar and non-polar fractions of core section 13A-3.

Figure 3-14 shows the steroid/hopanoid ratios across the depth of core section 13A-3, which preserves the mixing event. In the polar samples, the ratio does not change over depth in any noticeable pattern. However, the ratio in the nonpolar samples begins a sharp decrease at 147 cm and then stays approximately the same small value from 144.25 cm up to 135.25 cm. The pattern observed in the nonpolar samples reveals that the abundance of hopanoids significantly increases relative to the abundance of steroids across and throughout the mixing event. Notably, the total range of ratio values is much smaller in the polar samples than in the nonpolar samples.

3.4 Other Identified Compounds

In addition to the compound classes mentioned above, several other compounds were identified consistently throughout the samples. These include squalene, a compound associated with both sterol and hopanoid biosynthesis [3], and polycyclic aromatic

hydrocarbons (PAHs), compounds associated with incomplete combustion of fossil fuels. PAHs can be formed through a wide variety of processes, including through volcanic sources [5].

Chapter 4

Discussion

The primary purpose of this project is to shed further light on potential biological involvement in the proposed nitrogen cycling mechanism in Lake Kivu. We began by conducting a broad survey of the biomarkers present in the sediment samples. By calculating the relative abundances of compounds within samples relative to the largest peak present in each sample, we were able to broadly view the changes in compound class (alka(e)ne, steroid, hopanoid) prevalence across depth. There were several areas of interest in the heat maps, particularly in those from core section 13A-3. In the non-polar fraction, these areas of interest were: the diatomite layers (boxed in green), the mixing event (boxed in red), and the consistent presence of Cholest-2-ene (boxed in orange).

The diatomite layers show a higher relative abundance of alka(e)nes compared to the surrounding depths. While many organisms are capable of producing fatty acids, diatoms are a major source of such compounds and so an alka(e)ne-rich sample is consistent with a diatomite layer [13]. Diatoms are present across all layers of Lake Kivu; although the presence of abundant n-alka(e)nes may be consistent with the presence of diatoms, it does not reveal the layer of origin of the organisms. The diatomite's presence within the mixing event does imply an oxic layer origin but the

biomarker data can neither confirm nor deny this claim.

The non-polar fraction, particularly from core sample 3A, also showed a consistently high relative abundance of a steroidal compound, later determined to be Cholest-2-ene. Cholest-2-ene, a C₂₇ sterene, can derive from a number of sources, including zooplankton and diatoms. Lake Kivu does have a documented zooplankton population [1] and, given the presence of the aforementioned diatomite layers, diatom sources are also a reasonable option. Thus, it is not possible to distinguish between the two sources based solely on the data presented in this paper. Further identification of sterenes could prove useful; previous studies show that an equal distribution of C₂₇, C₂₈, and C₂₉ sterenes supports a diatom source over a zooplankton source [9].

Finally, the non-polar fraction from core sample 3A shows a noticeable increase in the relative abundance of hopanoids at the beginning of the mixing event (Figure 3-6) that continued for several centimeters. The calculated steroid/hopanoid ratios (Figure 3-14) further supports the argument for an increased abundance of hopanoids. The value of the ratio reaches a peak at a depth of 147 cm and then quickly drops to below 2, where it remains for the entirety of the mixing event and successive layers. The low ratio reveals an increasing amount of hopanoids relative to steroids. The polar fraction surrounding the mixing event shows a similar increase in hopanoid relative abundance, although there are also two hopanol compounds found in the fraction that have relatively high and consistent abundances throughout the entire depth of the section. As mentioned earlier, hopanoid biomarkers are typically associated with bacterial sources. The bacterial population of Lake Kivu is extensive, with some of the most abundant groups being shown in Figure 4-1.

Phylogenetic group	Num.OTUs	Oxic layer ^b (0–30 m)	Oxic-anoxic transition	Anoxic layer (50–100 m)
Bacteria				
<i>Actinobacteria</i>	1	+	+	+
<i>Bacteroidetes</i>	3	+	+	–
<i>Betaproteobacteria</i>	2	+	+	+
<i>Firmicutes/Clostridium</i>	2	+	–	+
<i>Nitrospira</i>	1	+	+	–
<i>Deltaproteobacteria</i>	1	–	–	+
<i>Mollicutes</i>	1	–	–	+
<i>Chlorobi</i>	1	–	–	+
Archaea^a				
Euryarchaeota				
<i>Methanosaeta</i>	4	+	+	+
<i>Methanocella</i>	1	–	+	–
<i>Thermoplasmata</i>	1	–	–	+
<i>DHVE-5</i>	1	–	–	+
Thaumarchaeota				
<i>Marine 1.1a</i>	1	+	+	–
<i>Soil 1.1b</i>	11	+	+	+
Crenarchaeota				
<i>C3</i>	2	–	+	+
<i>MCG</i>	6	–	+	+
<i>tMCG</i>	1	–	–	+

Figure 4-1: The bacterial and archaeal species present in Lake Kivu across layers [6].

When attempting to determine the source of hydrocarbon biomarkers, carbon isotope data can also be helpful. While this project did not involve sample-specific carbon isotope determinations, previous work did determine bulk carbon isotope values across the mixing event. At a depth of 145 cm in the sediment core used for this study, the $\delta^{13}\text{C}$ value is approximately -31. As seen in Figure 4-2, this $\delta^{13}\text{C}$ value is associated with freshwater plankton.

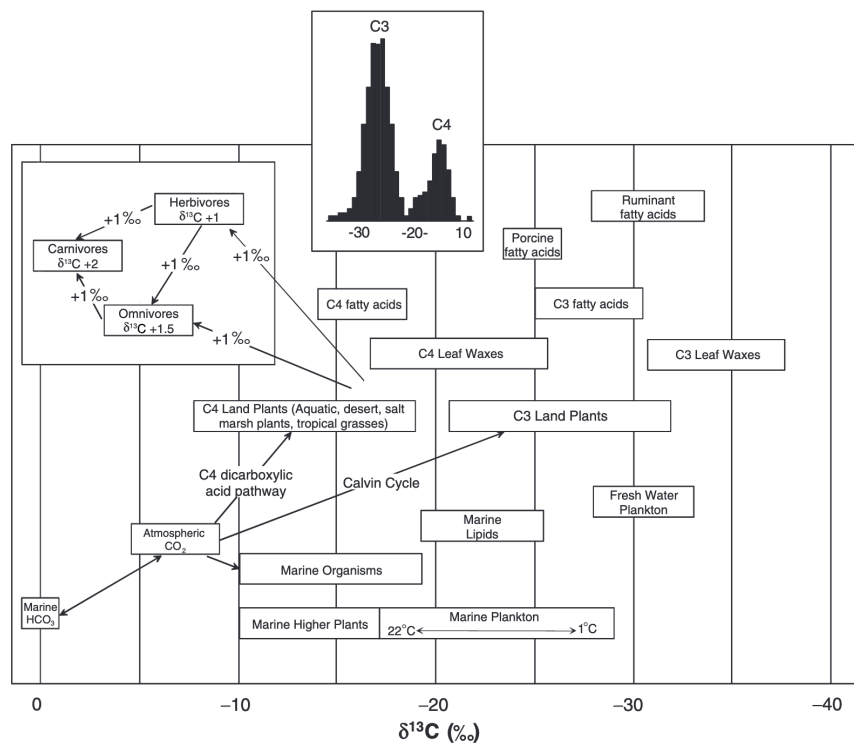


Figure 4-2: The organisms and compounds associated with various $\delta^{13}\text{C}$ values [10].

Chapter 5

Conclusion

The proposed nitrogen cycling mechanism centers around the idea that ^{15}N -depleted biomass is deposited on the lakebed following the upward transport of NH_4^+ . The biomarkers detected in the sediment samples are consistent with the microbial population known to exist within Lake Kivu, both in the photic zone and in the deep anoxic layers. However, the data taken from the depths associated with the mixing event is significantly different than the data associated with other depths of the sediment sample. It shows significant organic matter deposits and the biomarkers identified further reveal diatoms, bacteria, and zooplankton as potential sources. All three groups are present in the oxic, uppermost layer of Lake Kivu. Thus, the data presented is consistent with a biologically mediated nitrogen cycling mechanism. The proposed mechanism gains more credence when previously collected data, such as carbon isotope values and detected carotenoid and chlorophyll biomarkers, are considered.

There is a great deal of further work that could be done to address the question in more detail. If the mass spectrometry data were to be analyzed more closely and more specific compound identifications were made, organism-specific claims about the microbial community surrounding the mixing event might be possible. Additionally, it

would be useful to analyze data from more sampling sites. While all of these sediment samples came from one core, many others were collected and are able to be searched for biomarkers. The core from site 13-4AB is thought to preserve the same mixing event but at a different depth and early data does show a similar $\delta^{15}\text{N}$ excursion. Collecting data from that site would make an important comparison possible and create an initial understanding of what data are characteristic of these sorts of nitrogen mixing events as opposed to being site-specific occurrences.

An understanding of the nitrogen cycling mechanisms in Lake Kivu is important not only for a better understanding of Kivu's ecosystem, but also as an analogue for Ocean Anoxic Events. Although many aspects of OAEs remain poorly understood, we are making great strides in our understanding of characteristic $\delta^{15}\text{N}$ excursions. With further study of analogous environments such as Lake Kivu, these questions can be fully answered.

Appendix A

Figures

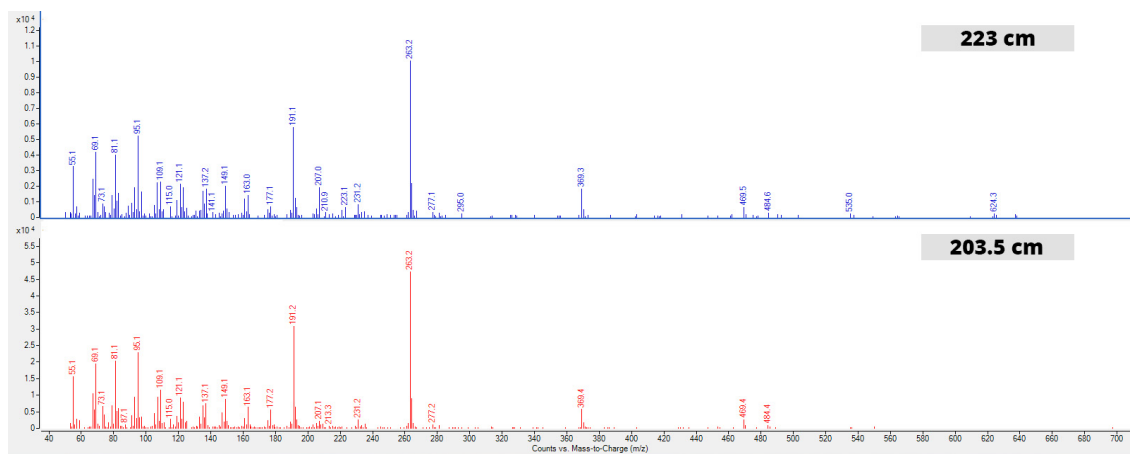


Figure A-1: Mass spectra from the polar fraction of core sample 4A that eluted at approximately 100 minutes.

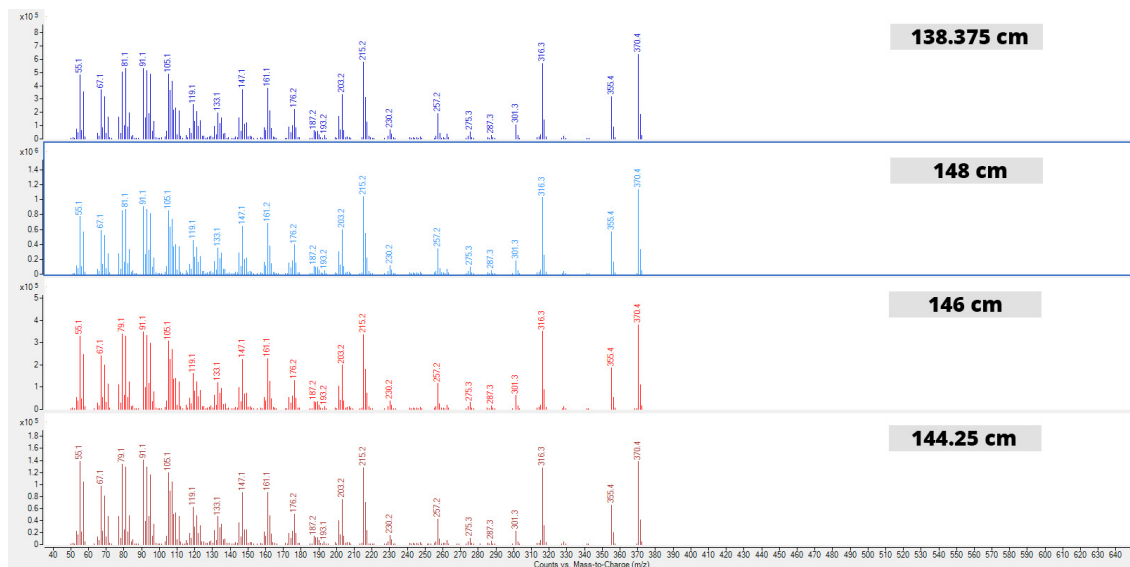


Figure A-2: Mass spectra from the non-polar fraction of core sample 3A showing a steroid, identified as Cholest-2-ene, that eluted at approximately 70 minutes.

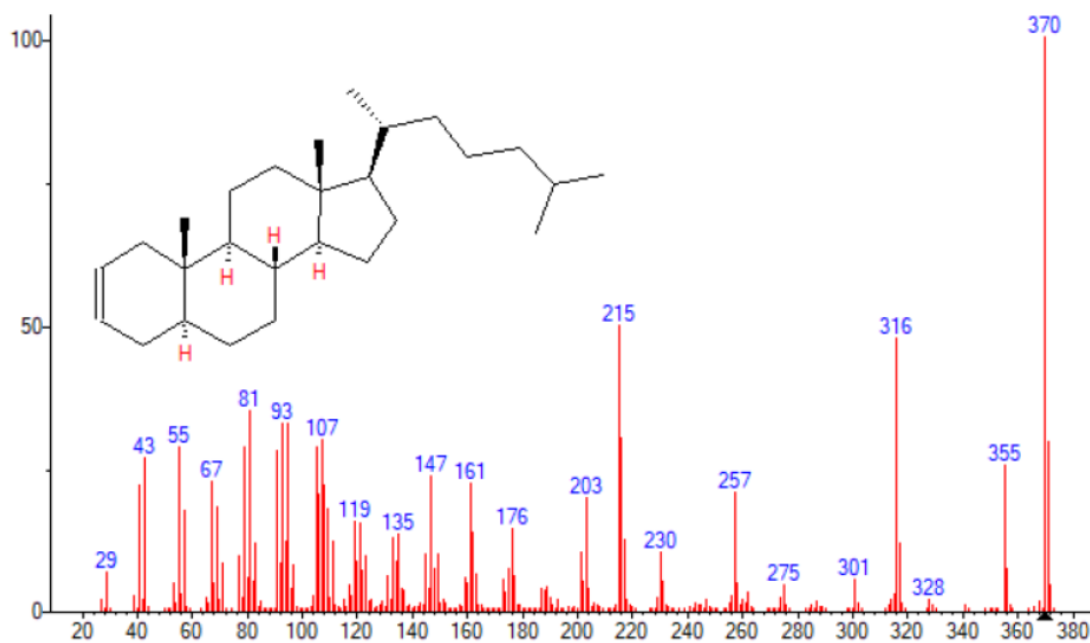


Figure A-3: Reference spectrum for Cholest-2-ene.

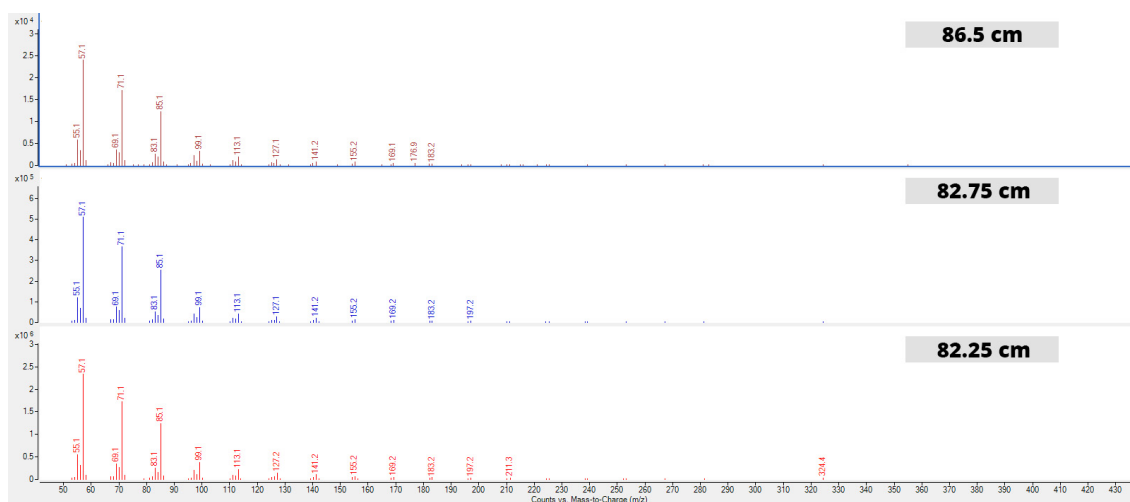


Figure A-4: Mass spectra from the non-polar fraction of core sample 2A showing an n-alkane that eluted at approximately 58 minutes.

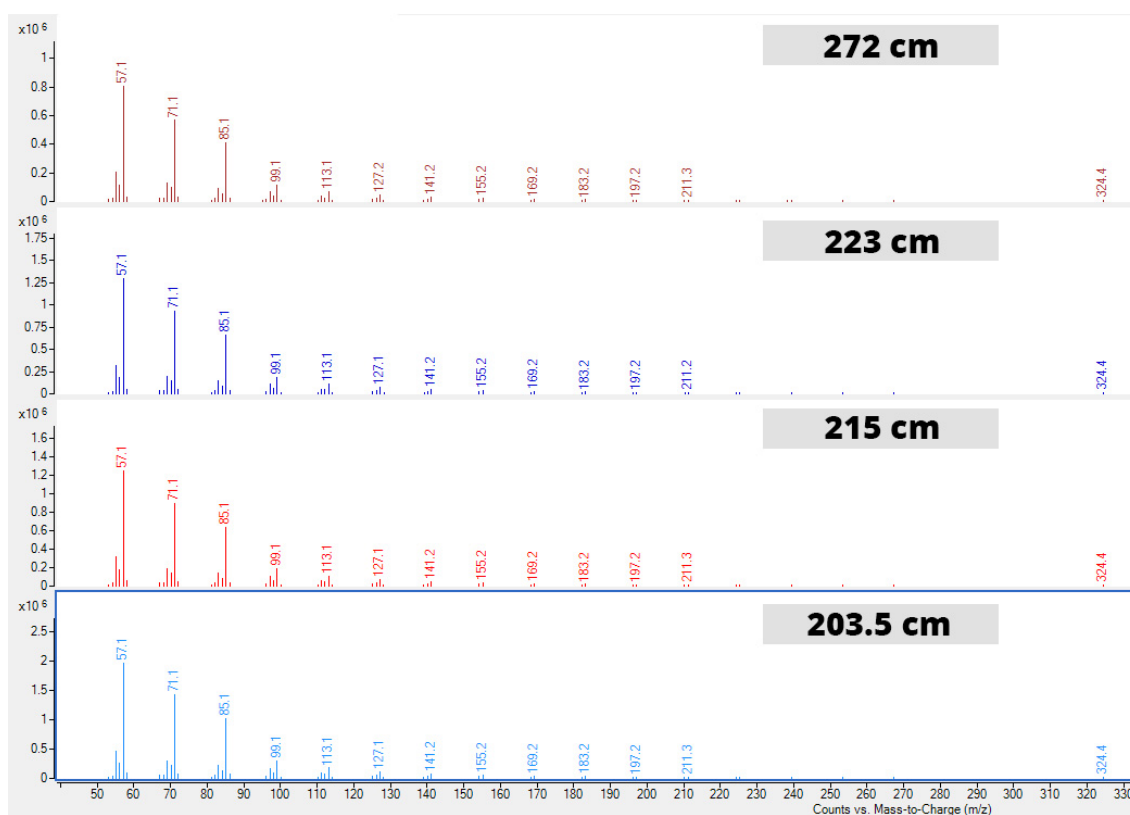


Figure A-5: Mass spectra from the non-polar fraction of core sample 4A showing an n-alkane that eluted at approximately 58 minutes.

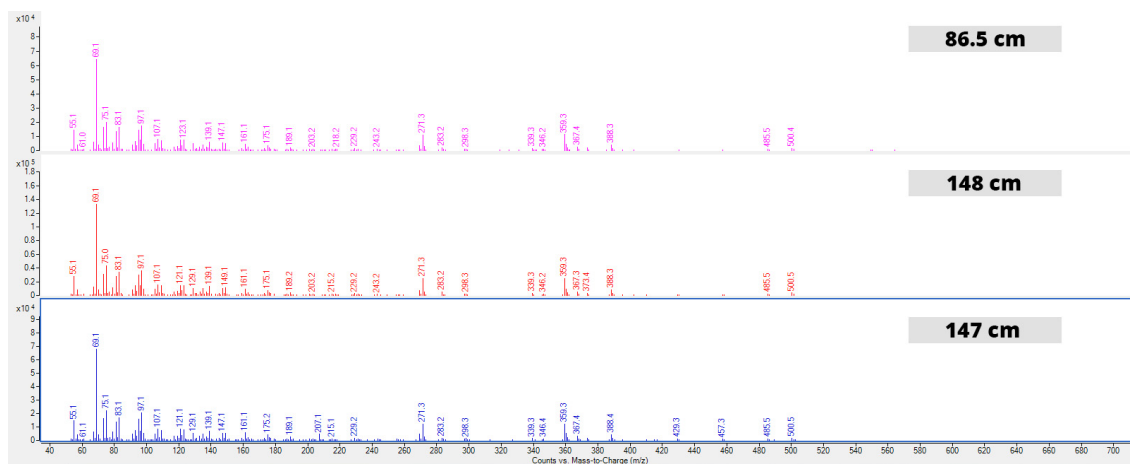


Figure A-6: Mass spectra from the polar fraction of core samples 2A and 3A that eluted at approximately 80 minutes.

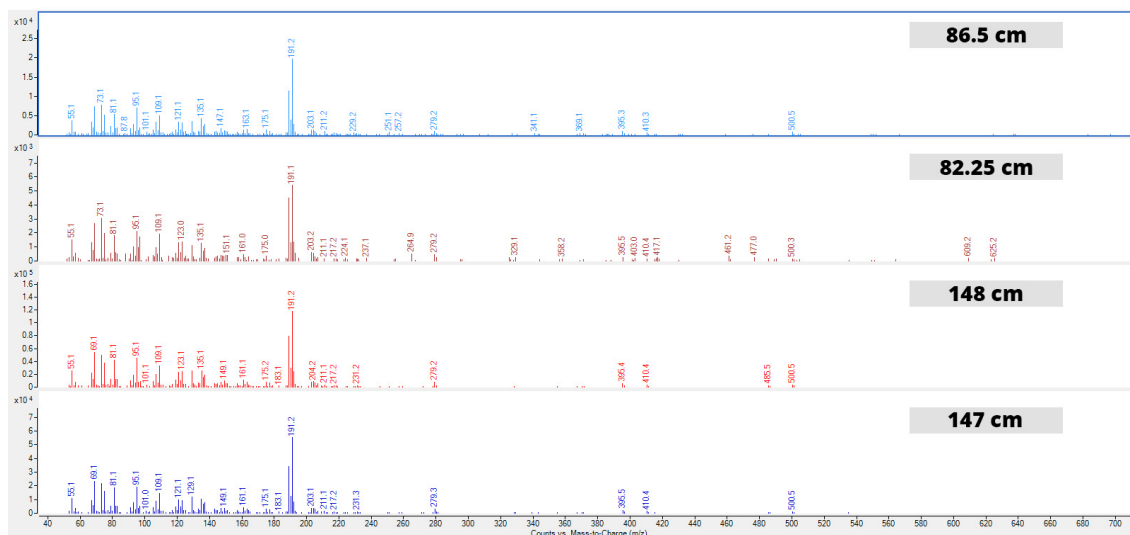


Figure A-7: Mass spectra from the polar fraction of core samples 2A and 3A that eluted at approximately 86 minutes.

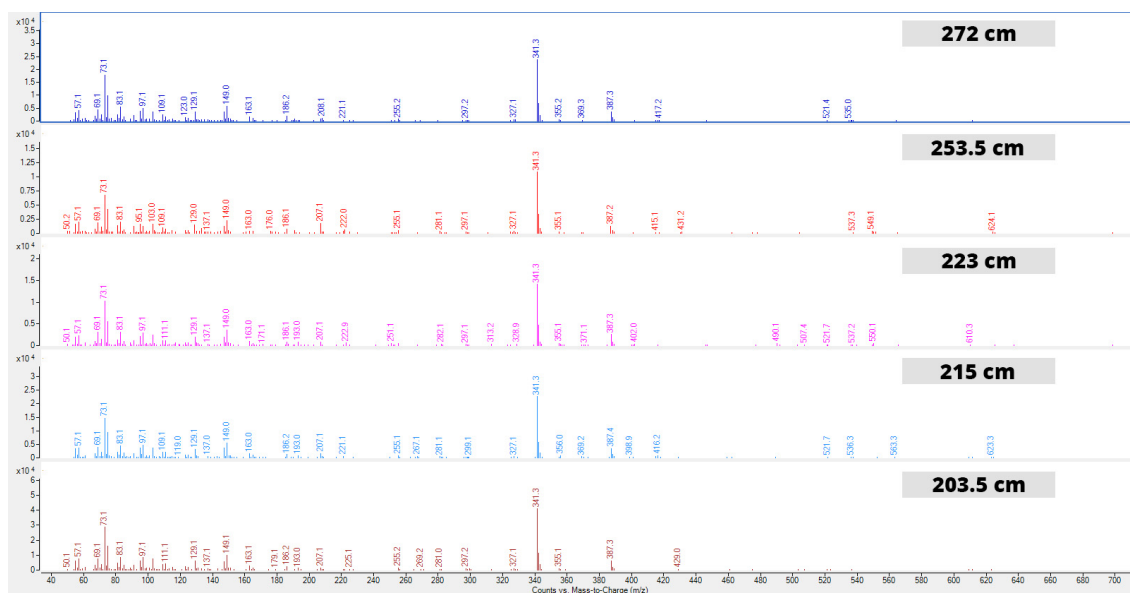


Figure A-8: Mass spectra from the polar fraction of core sample 4A that eluted at approximately 89 minutes.

Bibliography

- [1] François Darchambeau, Mwapu Isumbisho, and Jean-Pierre Descy. Zooplankton of Lake Kivu. In Jean-Pierre Descy, François Darchambeau, and Martin Schmid, editors, *Lake Kivu*, pages 107–126. Springer Netherlands, Dordrecht, 2012.
- [2] Jean-Pierre Descy, François Darchambeau, and Martin Schmid, editors. *Lake Kivu*. Springer Netherlands, Dordrecht, 2012.
- [3] Geoffrey F. Gibbons, L. John Goad, T.W. Goodwin, and William R. Nes. Concerning the Role of Lanosterol and Cycloartenol in Steroid Biosynthesis. *Journal of Biological Chemistry*, 246(12):3967–3976, June 1971.
- [4] Hugh C. Jenkyns. Geochemistry of oceanic anoxic events: REVIEW. *Geochemistry, Geophysics, Geosystems*, 11(3):n/a–n/a, March 2010.
- [5] Katarzyna Kozak, Marek Ruman, Klaudia Kosek, Grzegorz Karasiński, Łukasz Stachnik, and Żaneta Polkowska. Impact of Volcanic Eruptions on the Occurrence of PAHs Compounds in the Aquatic Ecosystem of the Southern Part of West Spitsbergen (Hornsund Fjord, Svalbard). *Water*, 9(1):42, January 2017.
- [6] Marc Llirós, Jean-Pierre Descy, Xavier Libert, Cédric Morana, Mélodie Schmitz, Louise Wimba, Angélique Nzavuga-Izere, Tamara García-Armisen, Carles Borrego, Pierre Servais, and François Darchambeau. Microbial Ecology of Lake Kivu. In Jean-Pierre Descy, François Darchambeau, and Martin Schmid, editors, *Lake Kivu*, pages 85–105. Springer Netherlands, Dordrecht, 2012.
- [7] Marc Llirós, Frederic Gich, Anna Plasencia, Jean-Christophe Auguet, François Darchambeau, Emilio O. Casamayor, Jean-Pierre Descy, and Carles Borrego. Vertical distribution of ammonia-oxidizing crenarchaeota and methanogens in the epipelagic waters of lake kivu (rwanda-democratic republic of the congo). *Applied and Environmental Microbiology*, 76(20):6853–6863, 2010.
- [8] Katja M. Meyer and Lee R. Kump. Oceanic Euxinia in Earth History: Causes and Consequences. *Annual Review of Earth and Planetary Sciences*, 36(1):251–288, May 2008.
- [9] Anais Pagès, Kliti Grice, David T. Welsh, Peter T. Teasdale, Martin J. Van Kraendonk, and Paul Greenwood. Lipid Biomarker and Isotopic Study of Community Distribution and Biomarker Preservation in a Laminated Microbial Mat

from Shark Bay, Western Australia. *Microbial Ecology*, 70(2):459–472, August 2015.

- [10] Kenneth E. (Kenneth Eric) Peters. *The biomarker guide. 1, Biomarkers and isotopes in the environment and human history*. Cambridge University Press, Cambridge, second edition. edition, 2005.
- [11] Kelly Ann Ross, Benoît Smets, Marc De Batist, Michael Hilbe, Martin Schmid, and Flavio S. Anselmetti. Lake-level rise in the late Pleistocene and active subaquatic volcanism since the Holocene in Lake Kivu, East African Rift. *Geomorphology*, 221:274–285, 2014.
- [12] Benjamin T. Uveges, Christopher K. Junium, Christopher A. Scholz, and James M. Fulton. Chemocline collapse in Lake Kivu as an analogue for nitrogen cycling during Oceanic Anoxic Events. *Earth and Planetary Science Letters*, 548:116459, October 2020.
- [13] John K Volkman, Stephanie M Barrett, Susan I Blackburn, Maged P Mansour, Elisabeth L Sikes, and François Gelin. Microalgal biomarkers: A review of recent research developments. *Organic Geochemistry*, 29(5-7):1163–1179, November 1998.